Cell Stem Cell
Article

Infection-Responsive Expansion of the Hematopoietic Stem and Progenitor Cell Compartment in Zebrafish Is Dependent upon Inducible Nitric Oxide

Christopher J. Hall,[1] Maria Vega Flores,[1] Stefan H. Oehlers,[1] Leslie E. Sanderson,[1] Enid Y. Lam,[1] Kathryn E. Crosier,[1] and Philip S. Crosier[1,*]
[1]Department of Molecular Medicine and Pathology, School of Medical Sciences, The University of Auckland, Private Bag 92019, Auckland, New Zealand
*Correspondence: ps.crosier@auckland.ac.nz
DOI 10.1016/j.stem.2012.01.007

SUMMARY

Hematopoietic stem cells (HSCs) are rare multipotent cells that contribute to all blood lineages. During inflammatory stress, hematopoietic stem and progenitor cells (HSPCs) can be stimulated to proliferate and differentiate into the required immune cell lineages. Manipulating signaling pathways that alter HSPC capacity holds great promise in the treatment of hematological malignancies. To date, signaling pathways that influence HSPC capacity, in response to hematopoietic stress, remain largely unknown. Using a zebrafish model of demand-driven granulopoiesis to explore the HSPC response to infection, we present data supporting a model where the zebrafish ortholog of the cytokine-inducible form of nitric oxide synthase (iNOS/NOS2) Nos2a acts downstream of the transcription factor C/ebpβ to control expansion of HSPCs following infection. These results provide new insights into the reactive capacity of HSPCs and how the blood system is "fine-tuned" in response to inflammatory stress.

INTRODUCTION

As the progenitors of all blood lineages, HSCs remain largely quiescent and only enter the cell cycle when required to contribute differentiated progeny. Recently, it has emerged that the HSC compartment and their more short-lived multipotent progeny (collectively termed hematopoietic stem and progenitor cells [HSPCs]) can directly react to inflammatory stress by proliferating and differentiating into the required cellular progeny (Baldridge et al., 2011; King and Goodell, 2011; Takizawa et al., 2011). Factors that influence HSPC capacity hold promise in improving ex vivo HSPC expansion for engraftment in patients with hematologic malignancies (Dahlberg et al., 2011). Promoting quiescent HSCs to enter the cell cycle, by inducing hematopoietic stress with inflammatory cytokines, has also been proposed as a potential mechanism of sensitizing dormant leukemic stem cells to the antiproliferative activities of chemotherapeutic agents (Trumpp et al., 2010). In light of these therapeutic applications, identifying novel pathways that expand/activate HSPCs is an area of intense interest.

During infection, consumption of neutrophils drives a demand-driven granulopoietic response within the bone marrow to facilitate their replenishment, often at the expense of other blood lineages (Panopoulos and Watowich, 2008; Ueda et al., 2005). This hematopoietic response also involves reactive proliferation/expansion of the HSPC compartment (Baldridge et al., 2010). Examining blood development in the context of inflammation and infection has resulted in the discovery of a number of immune mediators that drive demand-driven granulopoiesis and influence HSPC function (Baldridge et al., 2010, 2011; Hirai et al., 2006; Panopoulos and Watowich, 2008; Scumpia et al., 2010; Zhang et al., 2010). Well-characterized proinflammatory cytokines such as TNF-α and IFN-γ have been demonstrated to directly influence HSCs as part of a feedback loop, in response to depleted differentiated progeny (Baldridge et al., 2010; Rezzoug et al., 2008). Granulocyte colony-stimulating factor (G-CSF/CSF3) and its receptor G-CSFR/CSF3R are essential for both steady-state and stress-induced granulopoiesis (Panopoulos and Watowich, 2008). This granulopoiesis-promoting activity of G-CSF in response to infection is driven by the CCAAT enhancer binding protein, C/EBPβ (Hirai et al., 2006; Zhang et al., 2010). Signaling components that help regulate demand-driven neutrophil production, downstream of C/EBPβ, remain unknown.

In zebrafish (*Danio rerio*) the first bona fide HSCs emerge from hemogenic endothelial cells lining the ventral dorsal aorta (DA) from ~30 hr post fertilization (hpf). These endothelial cell-derived nascent HSCs transiently occupy the subaortic mesenchyme, a site analogous to the mammalian aorta-gonad-mesonephros (AGM) region, where they have been observed to undergo limited (i.e. a single), presumably symmetric cell division (Bertrand et al., 2010; Kissa and Herbomel, 2010; Lam et al., 2010). These blood progenitors are believed to maintain an HSC identity as they enter the circulation through the underlying cardinal vein and home to the caudal hematopoietic tissue (CHT) where they proliferate/differentiate before engrafting the definitive hematopoietic organs, the thymus and kidney (Murayama et al., 2006). Lineage tracing experiments suggest HSCs are only specified during this developmental window and no longer emerge de novo at later stages of development (Bertrand et al., 2010).

Employing a larval zebrafish model of demand-driven granulopoiesis to examine HSPC development through the "lens of infection," we provide new insight into how inflammatory stress "fine-tunes" hematopoiesis. We show that the zebrafish larval hematopoietic system responds to infection through the reactive expansion of the HSPC compartment. Further examination revealed a previously unappreciated role for C/ebpβ-dependent Nos2a-generated nitric oxide (NO) during HSPC and neutrophil-fated progenitor expansion following infection. These results provide new mechanistic insight into how the HSPC compartment responds to inflammatory stress.

RESULTS

Larval Hematopoietic Response to Infection

Prior to investigating the effect of infection on HSPCs, we examined whether larval hematopoiesis was responsive to infection. To address whether zebrafish replenish neutrophils lost as a result of cell death or apoptosis following infection, neutrophil abundance within *Tg(lyz:DsRED)* larvae (a transgenic reporter line that specifically marks neutrophils) was quantified throughout the course of infection. To facilitate direct observation of bacterial burden, a GFP-expressing *Salmonella enterica* serovar Typhimurium (hereafter referred to as Sal-GFP) was selected (Hall et al., 2007). Time-lapse imaging following injection of Sal-GFP into the hindbrain ventricle of *Tg(lyz:DsRED)* larvae at 50 hpf (Figure 1A) revealed robust recruitment of neutrophils to the midbrain and hindbrain. Highly motile neutrophils were observed phagocytosing the injected bacteria as part of an immediate innate immune response (Figure S1 and Movie S1, available online). One day following bacterial injection (1 dpi Infected), larvae demonstrated one of four phenotypes when compared with PBS-injected controls (1 dpi PBS). Infected larvae were: dead; overwhelmed by infection (such larvae never survived to 2 dpi and were always removed from further analysis); possessing numbers of neutrophils similar to uninjected controls that were dispersed throughout larval tissues (often with low levels of bacterial burden remaining in the head); or demonstrating a marked reduction in neutrophil numbers with very little or no detectable bacterial burden (Figure S1; see also Supplemental Experimental Procedures). Flow cytometry analysis revealing surviving larvae that possessed reduced neutrophil numbers at 1 dpi demonstrated a marked increase in whole-larvae neutrophil numbers that peaked at 2 dpi before gradually returning to steady-state levels, when compared with PBS controls (Figure 1B). We next examined whether this neutrophil expansion was the result of enhanced granulopoiesis within larval hematopoietic sites. Live imaging of infected larvae that possessed an almost complete loss of neutrophils by 1 dpi revealed de novo emergence of neutrophils within the AGM and CHT regions from 1.25–1.5 dpi that was most evident at 2 dpi (Figures 1C and 1D). All further assessment of infection on hematopoiesis focused on the AGM region (a region only sparsely populated with neutrophils under steady-state conditions) due to the confounding influence of steady-state granulopoiesis within the CHT. Throughout the remainder of this study (unless otherwise stated), an optimized infection dose of between 400 and 600 colony-forming units (cfu) was injected into the hindbrain ventricle at 50 hpf. This gave a sufficient proportion of larvae demonstrating neutrophil depletion at 1 dpi and subsequent demand-driven granulopoiesis, as scored within the AGM region at 2 dpi (~55% to 60% of surviving larvae), with survival of ~85% to 90% (Figure S1). Unless otherwise stated, data presented throughout the remainder of this study as "Infected" refers to this surviving cohort.

In support of our live imaging studies, quantitative-(Q)PCR analysis of the neutrophil-specific (*lyz* and *mpx*), pan-myeloid (*lcp1*), and myeloid progenitor (*spi1*) genes following infection demonstrated a peak in expression at ~2 dpi (Figure S1) (Lieschke et al., 2002; Lyons et al., 2001; Meijer et al., 2008). The macrophage-specific marker *csf1ra* also increased following infection, suggesting that demand-driven hematopoiesis may not be exclusively granulopoietic. To assess whether infection also resulted in expansion of the macrophage lineage, which shares a common *spi1*-expressing progenitor with neutrophils, we examined whether the macrophage-lineage marker *mpeg1* was also expressed by cells within the AGM following infection (Ellett et al., 2011). Although large numbers of macrophages were detected within the infection site, consistent with the later timing of macrophage infiltration during inflammation, no expression of *mpeg1* was observed within the AGM region (Figure 1E). This was in contrast to *spi1* expression, which strongly marked myeloid progenitors within this domain (Figure 1E). Expression analysis confirmed that these *spi1*-expressing progenitor cells were fated to the neutrophil lineage, as evidenced by *lyz* coexpression (Figure 1F).

To investigate whether demand-driven granulopoiesis influenced the development of the lymphoid lineage, we examined expression of the transcription factor *ikaros*, which typically marks lymphoid progenitors within the AGM, following infection at 2 dpi (Murayama et al., 2006; Willett et al., 2001) (Figure S1). Quantifying the number of somite boundaries within the AGM region containing *ikaros*$^{+}$ cells revealed a significant decrease in *ikaros* expression following infection (Figure S1). To examine if this decrease in *ikaros* expression resulted in a decrease in thymus-resident T cell precursors, we assessed the abundance of *lck*-expressing thymocytes within infected double transgenic *Tg(lck:GFP)/Tg(lyz:DsRED)* larvae at 3, 4, and 5 dpi, compared with PBS controls (Figure S1). Coincident with initiation of demand-driven granulopoiesis within the AGM and consistent with a decrease in *ikaros* expression, a marked decrease in *lck:GFP*-expressing thymocytes was observed following infection.

These results demonstrate that the larval zebrafish hematopoietic system can respond to infection by specifically enhancing the production of neutrophils, at the expense of other blood lineages.

Infected Larvae Possess an Expanded HSPC Compartment

To demonstrate that demand-driven granulopoiesis within the AGM was dependent upon definitive hematopoiesis (and by association resident HSPCs), we assessed the ability of Runx1-depleted embryos to replenish neutrophil numbers following infection. Runx1 is a transcription factor that in zebrafish, as in mammals, is absolutely required for HSPC development and definitive hematopoiesis (Lam et al., 2009). We have shown that HSPC ontogeny, including their emergence within

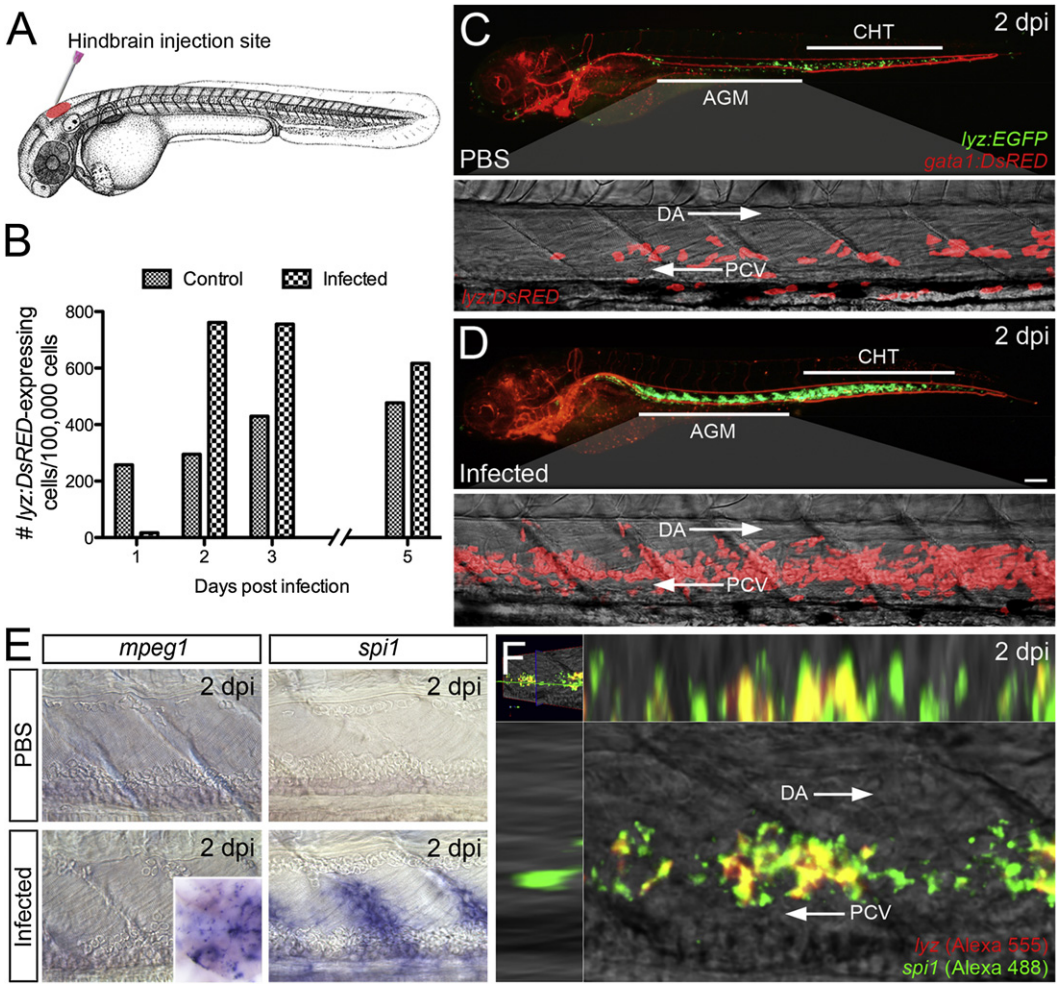

Figure 1. Larval Hematopoietic Response to Infection

(A) Schematic illustrating hindbrain injection site of live GFP-labeled *Salmonella*.

(B) Quantities of whole-larvae *lyz:DsRED*-expressing cells (per 100,000 sorted cells), as determined by flow cytometry, within infected *Tg(lyz:DsRED)* larvae (600 cfu) at 1, 2, 3, and 5 dpi, compared with PBS controls (n = 50 larvae/sample).

(C and D) Enhanced granulopoiesis within the AGM and CHT of infected (600 cfu) *Tg(lyz:EGFP)/Tg(gata1:DsRED)* larvae at 2 dpi, relative to PBS controls (with magnified views of AGM region within similarly treated *Tg(lyz:DsRED)* larvae). (B)–(D) refer only to those infected larvae that displayed neutrophil depletion at 1 dpi (see Supplemental Experimental Procedures).

(E) Expression of *mpeg1* and *spi1* within the AGM at 2 dpi following infection, compared with PBS controls. Inset demonstrates *mpeg1*-expressing cells within the midbrain and hindbrain.

(F) Dual WMISH of *lyz* and *spi1* expression within the AGM following infection at 2 dpi. All views, anterior to left.

Scale bar, 100 μm in (D). Abbreviations: AGM, aorta-gonad-mesonephros; CHT, caudal hematopoietic tissue; DA, dorsal aorta; PCV, posterior cardinal vein. See also Figure S1.

the subaortic mesenchyme of the AGM, can be observed within *Tg(runx1P2:EGFP)* embryos (Lam et al., 2010). Morpholino oligonucleotide (MO)-mediated depletion of Runx1 led to an almost complete absence of HSPCs within the AGM, decreased survival postinfection, and reduced steady-state granulopoiesis (Figure S2). Live imaging of double transgenic *Tg(lyz:DsRED)/Tg(runx1P2:EGFP)* larvae following infection revealed that Runx1/HSPC-depleted larvae did not initiate demand-driven granulopoiesis (Figure 2A). This suggested that demand-driven production of neutrophil-fated progenitors within the AGM develops by in situ differentiation from resident HSPCs. Of note, live imaging of infected *Tg(runx1P2:EGFP)* larvae revealed an increase in fluorescently marked HSPCs within the AGM following infection, a result supported by QPCR analysis of *runx1* expression (Figure S2) and validated by quantification of *cmyb*-expressing HSPCs within the AGM following infection (Figures 2B and 2C).

In mammals, although enriched in HSPCs, *c-myb* is also expressed within more committed blood cells (Kastan et al., 1989). In zebrafish, the earliest cells classified as HSCs are those that have directly differentiated from hemogenic endothelial cells (endothelial cells possessing hematopoietic potential) that line the ventral wall of the DA. Nascent HSCs then transiently occupy the subaortic mesenchyme between the main trunk vessels

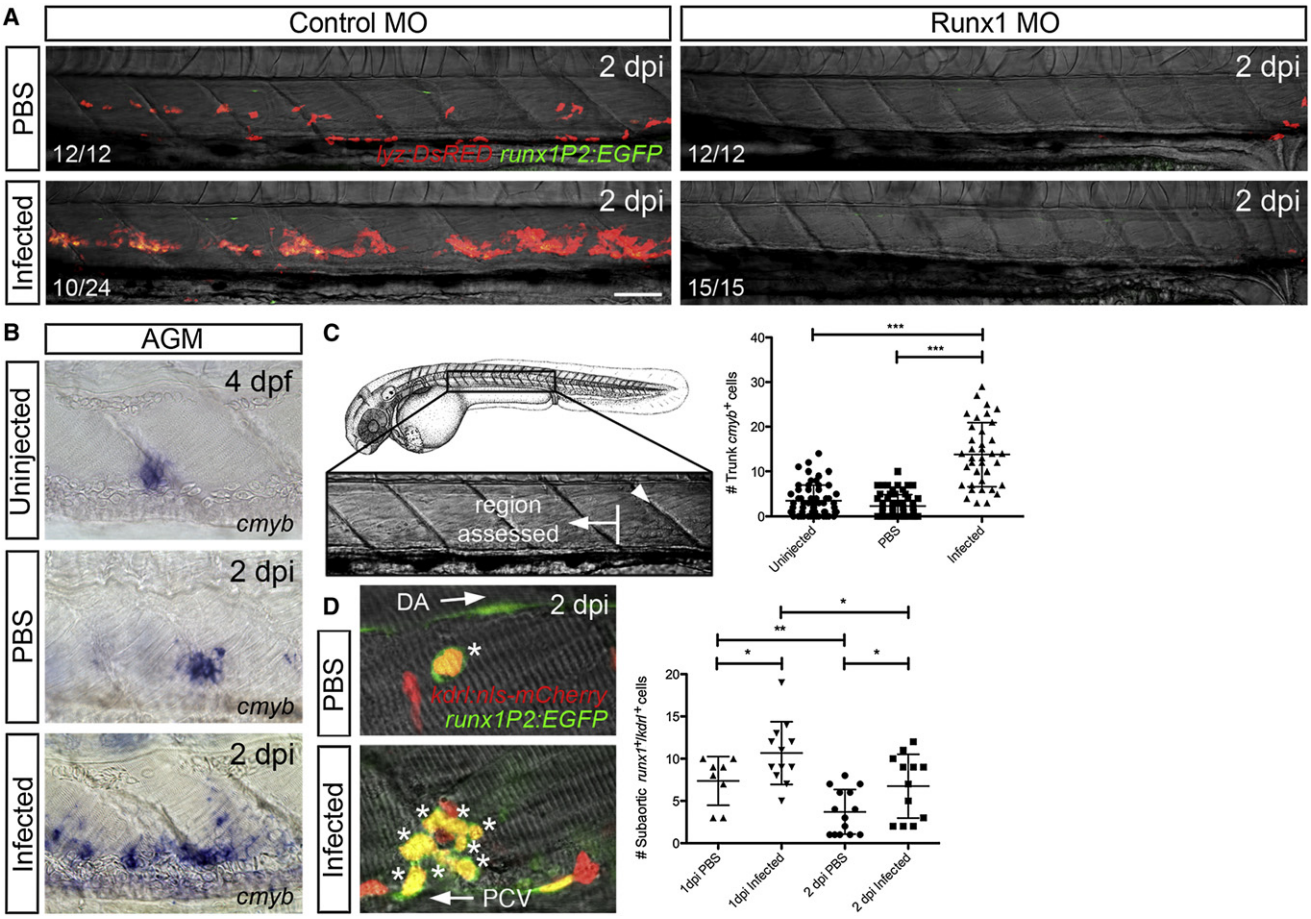

Figure 2. HSPC Compartment Expands in Response to Infection

(A) Confocal imaging through the AGM of control MO- and Runx1 MO-injected *Tg(lyz:DsRED)/Tg(runx1P2:EGFP)* larvae following infection, compared with PBS controls at 2 dpi.

(B) Expression of *cmyb* within the AGM of uninjected, PBS control and infected larvae at 2 dpi.

(C) Quantification of *cmyb*-expressing cells within the AGM (as defined in schematic) of larvae shown in (B); arrowhead marks somite boundary that intersects cloaca.

(D) Quantification of dual-labeled HSPCs (marked by asterisks) within the subaortic space of infected *Tg(runx1P2:EGFP)/Tg(kdrl:nls-mCherry)* larvae, compared with PBS controls at 1 and 2 dpi. All views, anterior to left. Numbers represent frequency of embryos or larvae with displayed phenotype.

Scale bar, 50 μm in (A). Abbreviations: DA, dorsal aorta; PCV, posterior cardinal vein; *$p < 0.05$; **$p < 0.01$; ***$p < 0.001$. See also Figure S2.

(Bertrand et al., 2010; Kissa and Herbomel, 2010). We have previously shown that subaortic *runx1*-expressing HSCs directly emerge from similarly *runx1*-expressing endothelial cells lining the ventral DA within compound *Tg(runx1P2:EGFP)/Tg(kdrl:nls-mCherry)* embryos (where the *kdrl:nls-mCherry* transgene marks endothelial nuclei with red fluorescence; Lam et al., 2010). Due to experimental limitations it is not possible to confirm whether all newly emerged progenitors maintain an HSC identity during their occupation of the subaortic mesenchyme and entry into the underlying vein. In light of this, we hereafter refer to these endothelial cell-derived subaortic *kdrl*$^+$*runx1*$^+$ blood progenitors (as marked within compound *Tg(runx1P2:EGFP)/Tg(kdrl:nls-mCherry)* larvae) as HSPCs. To confirm the effect of infection on the HSPC compartment, we quantified the number of dual fluorescent HSPCs within the subaortic region of infected *Tg(runx1P2:EGFP)/Tg(kdrl:nls-mCherry)* larvae, relative to PBS controls. This revealed an increase in HSPCs within the subaortic mesenchyme that could be detected by 1 dpi, immediately preceding the detection of *lyz*-expressing cells (Figure 2D). Of note, there was no difference in the number of *kdrl*$^+$*runx1*$^+$ endothelial cells between PBS control and infected larvae (Figure S2). This suggests that the increase in HSPC numbers following infection is not the result of an increase in *kdrl*$^+$*runx1*$^+$ endothelial cell numbers that subsequently bud to produce HSPCs. Infection-responsive HSPC expansion is most likely the result of enhanced proliferation of HSPCs within the subaortic mesenchyme following their endothelial to HSPC transition.

These results confirm that demand-driven granulopoiesis involves the infection-responsive expansion of HSPCs that contribute to the neutrophil lineage.

Demand-Driven Granulopoiesis Is Dependent upon Gcsf/Gcsfr Signaling and the Inflammation-Responsive Transcription Factor C/ebpβ

During infection, myelopoiesis-promoting cytokines are believed to reach the bone marrow hematopoietic niche via the circulation

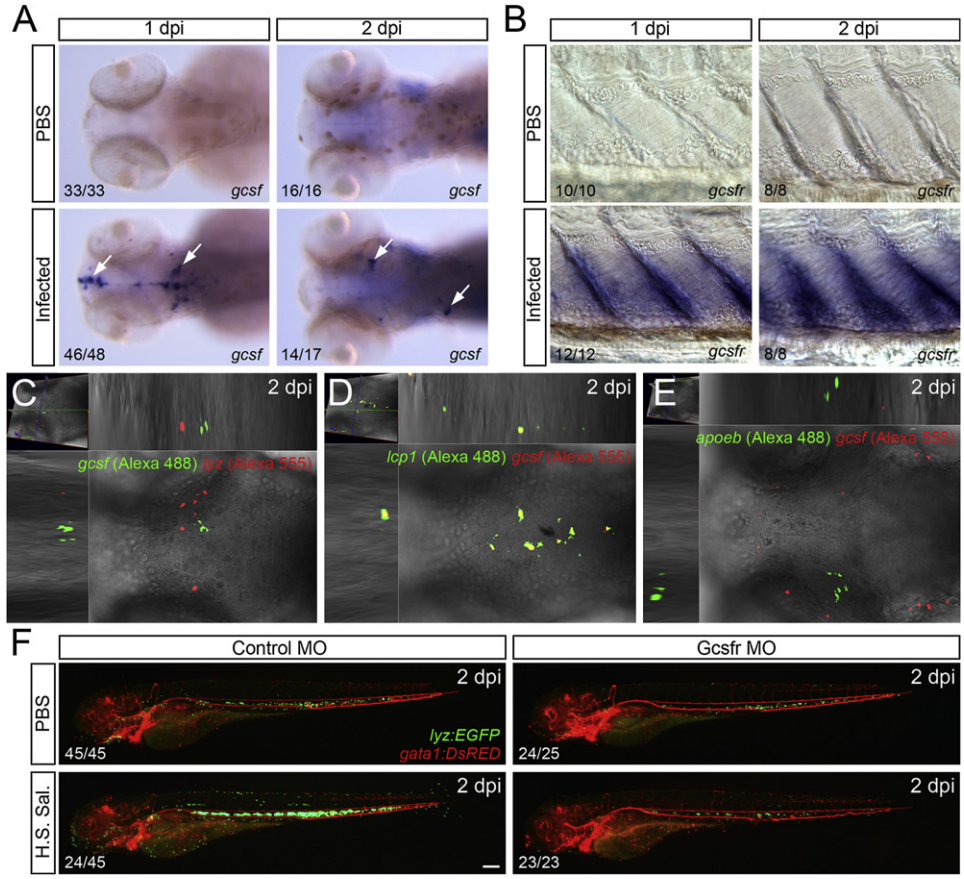

Figure 3. Demand-Driven Granulopoiesis Is Dependent upon Gcsf/Gcsfr Signaling

(A) Expression of *gcsf* within the midbrain and hindbrain of infected larvae (marked by arrows), dorsal views, compared with PBS controls at 1 and 2 dpi.
(B) Expression of *gcsfr* within the AGM of infected larvae, compared with PBS controls at 1 and 2 dpi.
(C–E) Dual WMISH of *gcsf* and *lyz*, and *lcp1* and *apoeb*, respectively, within the midbrain and hindbrain at 2 dpi following infection, with dorsal views shown.
(F) Control MO- and Gcsfr MO-injected *Tg(lyz:EGFP)/Tg(gata1:DsRED)* larvae following injection of heat-shocked *Salmonella* (H.S. Sal.), compared with PBS controls at 2 dpi. Numbers represent frequency of embryos or larvae with displayed phenotype.
Scale bar, 100 μm in (F). See also Figure S3.

to influence blood progenitor fate. G-CSF and macrophage colony-stimulating factor (M-CSF/CSF1) are the two predominant lineage-specific cytokines that drive neutrophil and macrophage production, respectively (Kaushansky, 2006; Motoyoshi, 1998). QPCR expression analysis of *csf1a*, *csf1b*, and *gcsf* transcripts following infection revealed that only *gcsf* demonstrated a significant elevation in expression that was coincident with demand-driven granulopoiesis (Figure S3). Whole-mount in situ hybridization (WMISH) analysis of *gcsf* revealed this expression to be restricted to the infection site (midbrain and hindbrain) while transcripts for its receptor, *gcsfr*, were detected within cells throughout the AGM compartment (Figures 3A and 3B). Given the lack of obvious *gcsfr* expression within HSPCs in the AGM region of control larvae, this elevated expression following infection is most likely a combination of enhanced expression within an expanded pool of HSPCs. Expression analysis revealed that all *lyz*-expressing neutrophils did not express *gcsf*, while all *gcsf*-expressing cells were positive for the pan-leukocyte marker *lcp-1* (Figures 3C and 3D). Furthermore, *gcsf*-expressing cells were not positive for the microglial marker *apolipoprotein Eb* (*apoeb*) (Figure 3E). The *lyz*$^{-}$*lcp1*$^{+}$ *apoeb*$^{-}$ phenotype is consistent with these *gcsf*-expressing cells being macrophages.

To address the requirement for Gcsf/Gcsfr signaling during demand-driven granulopoiesis, we infected Gcsfr-depleted double transgenic *Tg(lyz:EGFP)/Tg(gata1:DsRED)* larvae and assessed their ability to replenish neutrophils. Gcsfr-depleted larvae possessed fewer neutrophils and demonstrated reduced survival following infection when compared to control MO-injected siblings (Figure S3). Of note, Gcsfr-depleted larvae were more susceptible to infection than Runx1-depleted larvae, despite maintaining similar numbers of neutrophils at the time of infection. This suggests that the increased susceptibility to infection following Gcsfr depletion is largely the result of defective Gcsf/Gcsfr-mediated neutrophil function/maturation rather than reduced neutrophil numbers. This high susceptibility to infection following Gcsfr depletion precluded assessment of subsequent demand-driven granulopoiesis. To circumvent this, we injected nonlethal heat-shocked Sal-GFP, which, despite not depleting neutrophil numbers by 1 dpi, could still elicit

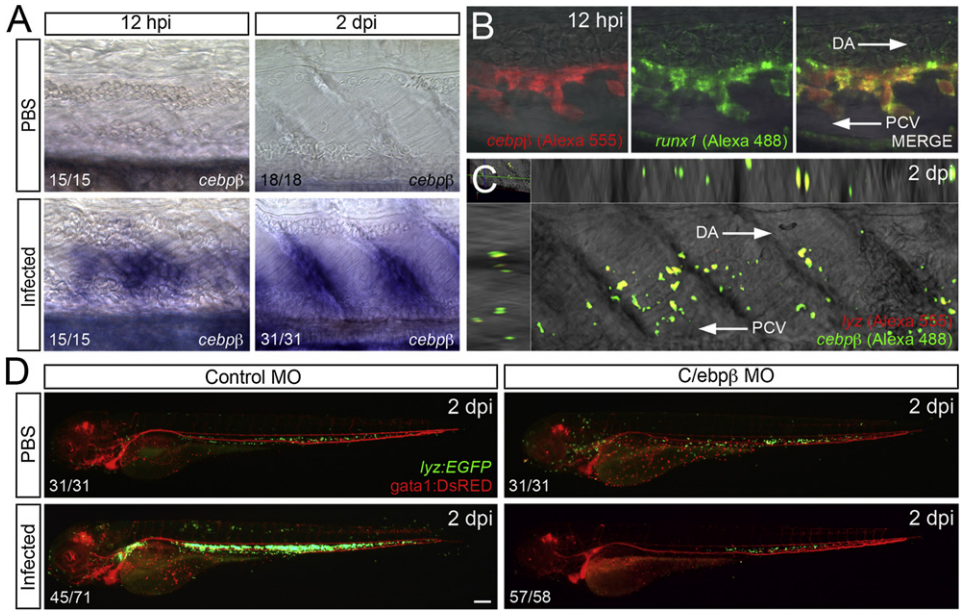

Figure 4. *cebpβ* Is Expressed within HSPCs in Response to Infection and Is Required for Demand-Driven Granulopoiesis

(A) Expression of *cebpβ* within the AGM of infected larvae, compared with PBS controls at 12 hpi and 2 dpi.

(B) Dual WMISH of *cebpβ* and *runx1* within the AGM of infected larvae at 12 hpi.

(C) Dual WMISH of *cebpβ* and *lyz* within the AGM of infected larvae at 2 dpi.

(D) Control MO- and C/ebpβ MO-injected *Tg(lyz:EGFP)/Tg(gata1:DsRED)* larvae following infection, compared with PBS controls at 2 dpi. Numbers represent frequency of embryos or larvae with displayed phenotype.

Scale bar, 100 μm in (D). All views, anterior to left. Abbreviations: DA, dorsal aorta; PCV, posterior cardinal vein. See also Figure S4.

a demand-driven granulopoietic response by 2 dpi, although not within Gcsfr-depleted larvae (Figure 3F and Figure S3).

These results confirm that Gcsf signaling is necessary for demand-driven expansion of *gcsfr*-expressing HSPCs within the AGM compartment. Of note, given that heat-killed bacteria maintained the capacity to initiate demand-driven granulopoiesis independent of the neutrophil depletion following live infection, neutrophil apoptosis appears to be dispensable for demand-driven granulopoiesis.

In mice, G-CSF-dependant demand-driven granulopoiesis is in part regulated by the downstream transcription factor C/EBPβ (Hirai et al., 2006; Zhang et al., 2010). A function for zebrafish C/ebpβ during hematopoiesis has not been reported. QPCR analysis of *cebpβ* expression revealed significant increases in expression coincident with the timing of demand-driven granulopoiesis (Figure S4). At both 12 hr postinfection (hpi) (prior to the demand-driven production of *lyz*-expressing cells) and 2 dpi, cells expressing *cebpβ* were detected within the AGM following infection (Figure 4A). Expression analysis revealed these earliest *cebpβ*-expressing cells in the AGM to be *runx1*$^{+}$ HSPCs, while later expression also included newly emerging *lyz*$^{+}$ neutrophil-fated progenitors (Figures 4B and 4C). Flow cytometry quantification of fluorescent neutrophils within C/ebpβ-depleted *Tg(lyz:DsRED)* embryos and larvae confirmed that this transcription factor, as in mammals, is dispensable for maintaining steady-state neutrophil numbers (Figure S4). This was in contrast to the situation following infection, where C/ebpβ MO-injected larvae were not able to replenish depleted neutrophil numbers, as demonstrated within double transgenic *Tg(lyz:EGFP)/Tg(gata1:DsRED)* larvae (Figure 4D).

These results strongly suggest that the transcription factor C/ebpβ, although dispensable for steady-state neutrophil production, is required within HSPCs and neutrophil-fated progenitors for their proliferation and/or differentiation into neutrophils during demand-driven granulopoiesis.

Nos2a Is Required for Demand-Driven Granulopoiesis and the Reactive Expansion of HSPCs following Infection

Downstream targets of C/EBPβ that promote demand-driven granulopoiesis following infection remain unknown. Predicted targets would be C/EBPβ responsive, demonstrate the potential to be modulated following immune stimulation, have the ability to influence hematopoiesis, and suppress apoptotic signals and/or enhance cell proliferation. These criteria led us to investigate a potential role for the cytokine-inducible form of NO (produced by NOS2/INOS), a well-characterized regulator of diverse inflammatory responses (Korhonen et al., 2005). The *nos2* gene is duplicated in zebrafish (*nos2a* and *nos2b*). Of these paralogs, Nos2a has been shown to more closely resemble mammalian NOS2 with regard to stress-induced properties (Lepiller et al., 2009). The zebrafish ortholog of Nos1 has been demonstrated to contribute to steady-state numbers of *runx1*/*cmyb*-expressing HSPCs within the AGM region, supporting a proliferative role for constitutive NO during HSPC development (North et al., 2009).

To first evaluate whether NOS activity was necessary for infection-responsive expansion of the neutrophil lineage, we exposed infected *Tg(lyz:DsRED2)* larvae to a number of pan-NOS and isoform-specific NOS inhibitors from 6 hpi. The pan-NOS

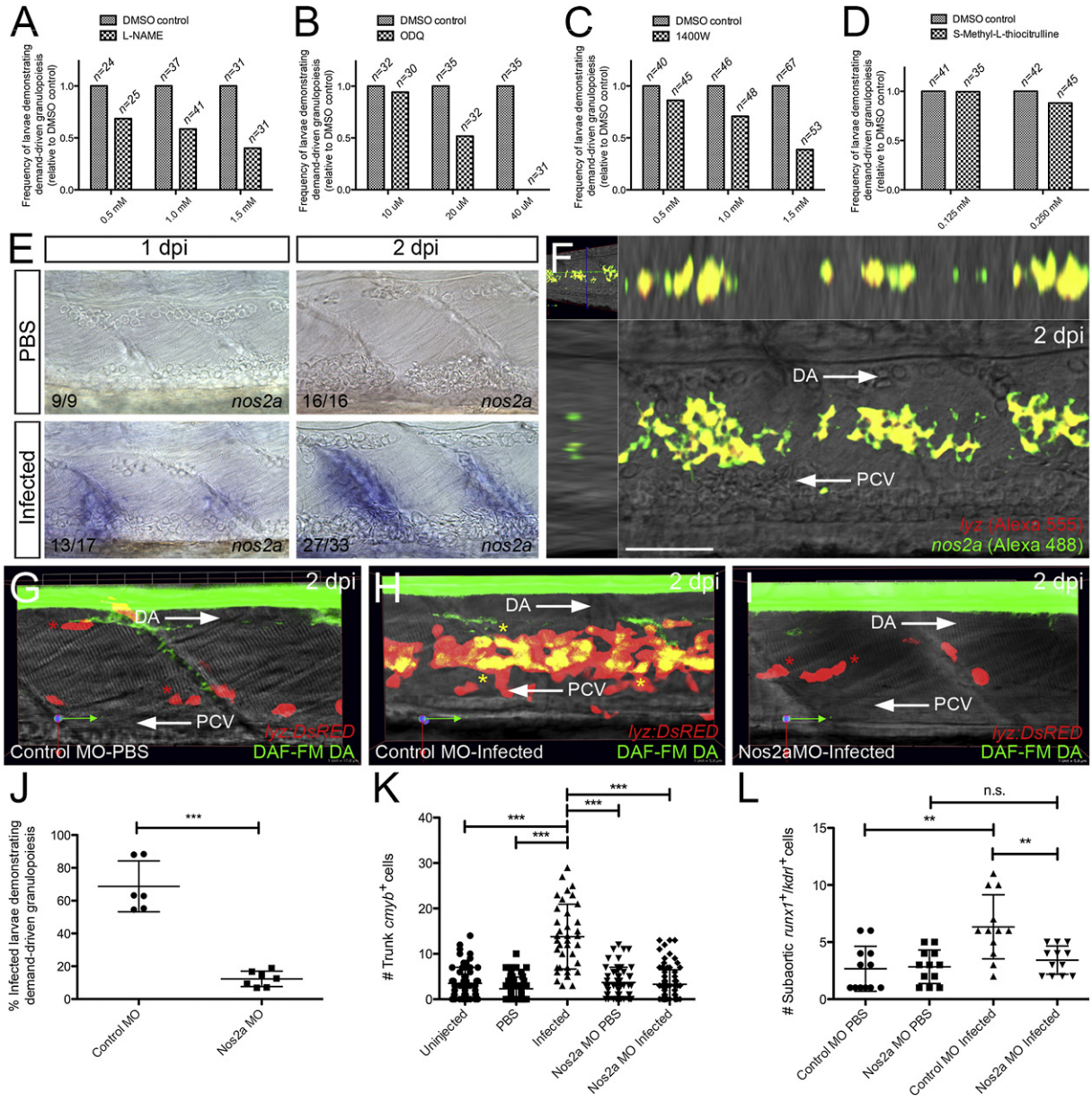

Figure 5. Demand-Driven Granulopoiesis and HSPC Expansion Are Dependent upon Nos2a

Relative frequency of infected larvae demonstrating demand-driven granulopoiesis following treatment (from 6 hpi) with the NOS inhibiting drugs L-NAME (A), ODQ (B), 1400W (C), and S-Methyl-L-thiocitrulline (D), all relative to DMSO control treatment. Numbers represent numbers of larvae in each treatment group. (E) Expression of *nos2a* within the AGM of infected larvae, compared with PBS controls at 1 and 2 dpi. (F) Dual WMISH of *nos2a* and *lyz* within the AGM of infected larvae at 2 dpi. (G–I) DAF-FM DA detection of NO within control MO-injected PBS control, control MO-injected infected, and Nos2a MO-injected infected *Tg(lyz:DsRED)* larvae, respectively, at 2 dpi. Yellow and red asterisks mark lyz^{+}/NO^{+} and lyz^{+}/NO^{-} cells, respectively. (J) Percentage of control MO- and Nos2a MO-injected *Tg(lyz:DsRED)* infected larvae demonstrating demand-driven granulopoiesis at 2 dpi. (K) Number of *cmyb*-expressing HSPCs, as detected by WMISH at 2 dpi, within the AGM compartment (as defined in Figure 2C) following indicated treatments. (L) Quantification of dual-labeled HSPCs within the subaortic space of 2 dpi *Tg(runx1P2:EGFP)/Tg(kdrl:nls-mCherry)* larvae following indicated treatments. Numbers represent frequency of embryos or larvae with displayed phenotype. All views, anterior to left. Scale bar, 50 μm in (F). Abbreviations: DA, dorsal aorta; PCV, posterior cardinal vein; n.s., not significant; $^{**}p < 0.01$; $^{***}p < 0.001$. See also Figure S5.

inhibitors L-NAME (Figure 5A) and L-NMMA (Figure S5), as well as the NO-sensitive guanylyl cyclase inhibitor ODQ (Figure 5B) and NOS2-specific inhibitor 1400W (Figure 5C), all resulted in a dose-dependent reduction in larvae demonstrating demand-driven granulopoiesis. This was in contrast to the nNOS/NOS1-specific inhibitor S-Methyl-L-thiocitrulline, which had no effect (Figure 5D). A temporal analysis of 1400W treatment demonstrated that the requirement for NOS2 was comparable with the timing of demand-driven granulopoiesis (Figure S5). Of note, treatment of PBS control-injected siblings with all drugs

used, at all doses, resulted in no observable developmental defects, including steady-state neutrophil production (data not shown). These results prompted us to evaluate the expression of *nos2a* within the AGM compartment following infection. Presumptive HSPCs expressing *nos2a* were detected as early as 1 day following infection (Figure 5E). Expression analysis at 2 dpi revealed that the majority of *nos2a*-expressing cells were *lyz*$^+$ neutrophil-fated progenitors (Figure 5F).

Next we exploited the live imaging potential of the cell-permeable 4-amino-5-methylamino-2′,7′-difluororescein diacetate (DAF-FM DA) fluorescent NO probe to examine whether this infection-responsive *nos2a* expression within the AGM correlated with active NO production. Consistent with the expression analysis, NO was detected within *lyz:DsRED*-expressing cells within the AGM compartment, specifically following infection (Figures 5G and 5H). To confirm a role for Nos2a during NO production and demand-driven granulopoiesis, we assessed NO production within Nos2a-depleted infected *Tg(lyz:DsRED)* larvae and the potential of Nos2a-depleted compound *Tg(lyz:EGFP)/Tg(gata1:DsRED)* larvae to replenish depleted neutrophil numbers following infection (Figures 5G–5J and Figure S5). This revealed a requirement for Nos2a during NO production and demand-driven granulopoiesis within the AGM following infection (Figures 5I and 5J and Figure S5). Flow cytometry quantification of fluorescent neutrophils within Nos2a-depleted *Tg(lyz:DsRED)* embryos and larvae confirmed that Nos2a, like C/ebpβ, was dispensable for maintaining homeostatic neutrophil numbers (Figure S5). No significant reduction in survival was observed within Nos2a-depleted larvae following infection, suggesting that Nos2a, although required for neutrophil replenishment/expansion in response to infection, was not required to survive the infection doses used in this study (Figure S5). Given the early expression of both *cebpβ* and *nos2a* by HSPCs within the AGM when HSPC numbers within this region are expanding, we investigated whether Nos2a was required for HSPC expansion following infection. This analysis revealed that the infection-responsive increases of both *cmyb*- and *runx1P2:EGFP/kdrl:nsl-mCherry*-expressing HSPCs within the subaortic mesenchyme are Nos2a-dependent (Figures 5K and 5L). These results confirm a role for Nos2a-generated NO during infection-responsive expansion of subaortic HSPCs.

Nos2a Functions Downstream of C/ebpβ during Demand-Driven Granulopoiesis

To establish a genetic link between C/ebpβ and Nos2a, we assessed the expression of each in the absence of the other, within the AGM compartment following infection (Figures 6A and 6B). This revealed a decrease in larvae expressing *nos2a* within the AGM following C/ebpβ-depletion while most infected Nos2a-depleted larvae maintained a reduced population of *cebpβ*-expressing cells (Figures 6A and 6B). Following infection, the abundance of *cebpβ*$^+$ cells within the AGM of Nos2a-depleted larvae at 2 dpi was similar to that detected at 1 dpi (Figure S6). This suggests that, in the absence of Nos2a, *cebpβ*-expressing HSPCs do not expand in number. To further support the positioning of C/ebpβ upstream of Nos2a, we first examined the potential of ectopic *cebpβ* to drive *nos2a* expression. Injection of *cebpβ* mRNA into one-cell stage zebrafish embryos resulted in a proportion of precirculation embryos possessing ectopic *nos2a* expression on the yolk surface (Figure 6C). Repeating this experiment within *Tg(lyz:EGFP)* embryos followed by triple fluorescent labeling to detect injected *cebpβ* (Alexa 488), *nos2a* (Alexa 555), and lyz:EGFP (Alexa 633) revealed that this ectopic *nos2a* expression was only observed within *lyz:EGFP*-marked cells overexpressing *cebpβ* (Figure 6D). Of note, neither *cebpβ* nor *nos2a* expression was detected on the yolk of 22 hpf uninjected siblings (data not shown). In zebrafish, early myeloid cells that populate the precirculation yolk surface are derived from anterior lateral plate mesoderm and are believed to possess an early myeloid progenitor cell phenotype with neutrophil and macrophage potential (Le Guyader et al., 2008). The number of these cells, as detected by *lyz:EGFP* expression, was significantly expanded following forced *cebpβ* expression in a Nos2a-dependent manner (Figures 6E–6H).

These results are consistent with C/ebpβ driving *nos2a* expression within early primitive myeloid cells where it promotes their proliferation/expansion. Forcing expression of *cebpβ* within the AGM region to assess a similar ability to drive *nos2a* expression and Nos2a-dependent HSPC proliferation/expansion within this definitive blood compartment was not technically feasible. Despite this, the dependence on C/ebpβ for *nos2a* expression within HSPCs in this region, the requirement of Nos2a for HSPC expansion, and the need for both during neutrophil progenitor expansion following infection supports a conserved relationship within the AGM compartment.

DISCUSSION

Using a zebrafish model of demand-driven granulopoiesis to explore the reactive capacity of the blood stem cell compartment to inflammatory stress, we reveal that C/ebpβ-dependent Nos2a-generated NO is necessary for HSPC and neutrophil-fated progenitor expansion in response to infection. We propose a model whereby elevated serum Gcsf, produced by macrophages at the infection site, stimulates Gcsf-responsive AGM-resident HSPCs to express the transcription factor C/ebpβ. C/ebpβ then drives Nos2a expression, which supports HSPC proliferation/expansion (Figure 7). Given that we show steady-state neutrophil production occurs normally in the absence of endogenous NO, suggesting that transcriptional control of neutrophil commitment is independent of NO, we believe Nos2a-generated NO is required for C/ebpβ-driven proliferation of HSPCs but dispensible for their neutrophil commitment.

Live imaging within transgenic reporter lines possessing differentially fluorescent endothelial and blood progenitor lineages has confirmed that nascent HSPCs emerge directly from endothelial cells lining the DA (Bertrand et al., 2010; Kissa and Herbomel, 2010; Lam et al., 2010). These endothelially derived blood stem cells, specified within the AGM compartment, are believed to provide the life-long supply of HSPCs (Bertrand et al., 2010). Using live imaging of infected *Tg(runx1P2:EGFP)/Tg(kdrl:nls-mCherry)* larvae, we demonstrate that Nos2a is required for the infection-responsive expansion of this subaortic cell population within the AGM region. We also show that *nos2a* continues to be expressed within an expanding pool of neutrophil-fated progenitors and can drive the expansion of early primitive myeloid progenitors. Our results suggest that following infection, the subaortic AGM region is populated with enhanced numbers of

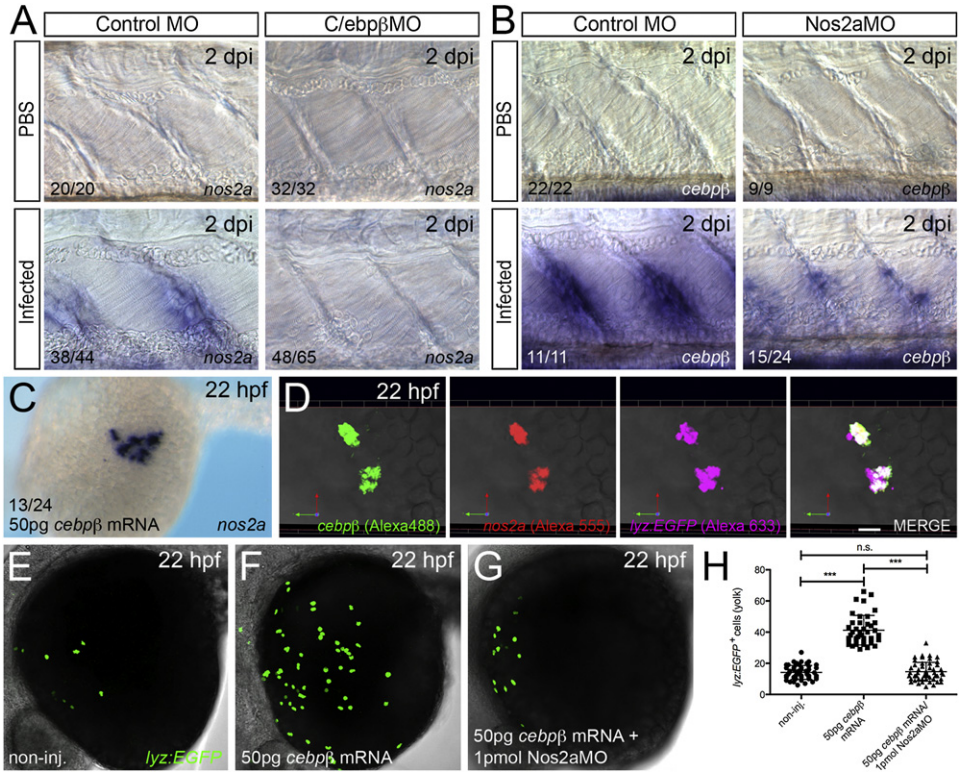

Figure 6. Nos2a Functions Downstream of C/ebpβ during Demand-Driven Granulopoiesis

(A) Expression of *nos2a* within the AGM of control MO- and C/ebpβ MO-injected larvae following infection, compared with PBS controls at 2 dpi.

(B) Expression of *cebpβ* within the AGM of control MO- and Nos2a MO-injected larvae following infection, compared with PBS controls at 2 dpi.

(C) Expression of *nos2a* at 22 hpf, following injection of 50 pg *cebpβ* mRNA.

(D) Dual WMISH of *cebpβ* and *nos2a* and immunofluorescence detection of lyz:EGFP within a *Tg(lyz:EGFP)* embryo at 22 hpf, following injection of 50 pg *cebpβ* mRNA.

(E–G) *lyz:EGFP*-expressing myeloid progenitors on the yolk of noninjected, *cebpβ* mRNA-injected, and *cebpβ* mRNA/Nos2a MO-injected *Tg(lyz:EGFP)* embryos at 22 hpf, respectively.

(H) Quantification of *lyz:EGFP*-expressing cells on the yolk of embryos in (E)–(G). Numbers represent frequency of embryos or larvae with displayed phenotype. All views, anterior to left. Scale bar, 10 μm in (D). Abbreviations: n.s., not significant; ***$p < 0.001$. See also Figure S6.

HSPCs that are becoming progressively restricted toward the neutrophil lineage. We believe that Nos2a acts at the level of the HSPC and their neutrophil-fated progenitor progeny to support proliferation in response to infection.

The attributes of the zebrafish we have exploited in this study, in particular its genetic tractability and optical transparency, restrict the use of this system to the embryonic and early larval stages of development. With this in mind we have used the zebrafish larval hematopoietic system as a surrogate for that in the adult. Our investigation into the larval hematopoietic response to infection has revealed a high degree of conservation with that reported within the mammalian bone marrow, in particular HSPC expansion, enhanced commitment toward the neutrophil lineage, and dependence on G-CSF signaling and C/EBPβ. Investigating HSPC development in embryonic zebrafish has resulted in unique insights into blood stem cell homeostasis that have been successfully translated to the adult mammalian blood system (North et al., 2007). Examining definitive hematopoiesis in embryonic and larval zebrafish has highlighted that many core signaling pathways and transcriptional networks that guide the development of the blood system also perform similar roles within the mammalian bone marrow to maintain blood cell homeostasis. In light of this, and given the conserved positive contribution of constitutive NO signaling during HSPC development within zebrafish and mice, we believe it is likely that the role of infection-responsive NO in promoting HSPC expansion we describe here will translate to the bone marrow compartment (Adamo et al., 2009; North et al., 2007).

During demand-driven granulopoiesis the transcription factor C/EBPβ functions downstream of G-CSF to couple differentiation and proliferation of neutrophil progenitors (Akagi et al., 2008; Hirai et al., 2006; Zhang et al., 2010). This is in contrast to steady-state neutrophil production where there is a model of mutual exclusion between proliferation and differentiation. We further resolve how the hematopoietic system responds to infection stress by demonstrating *cebpβ* expression, not only within neutrophil-fated precursors, but also within *runx1*$^{+}$ HSPCs where it promotes proliferation through a Nos2a-dependent mechanism. Studies have demonstrated a role for the *trans*-acting C/EBPβ in driving *NOS2* expression by direct binding to *cis*-acting elements in its promoter (Guo et al., 2003; Teng et al., 2002). We show that ectopic delivery of *cebpβ* can

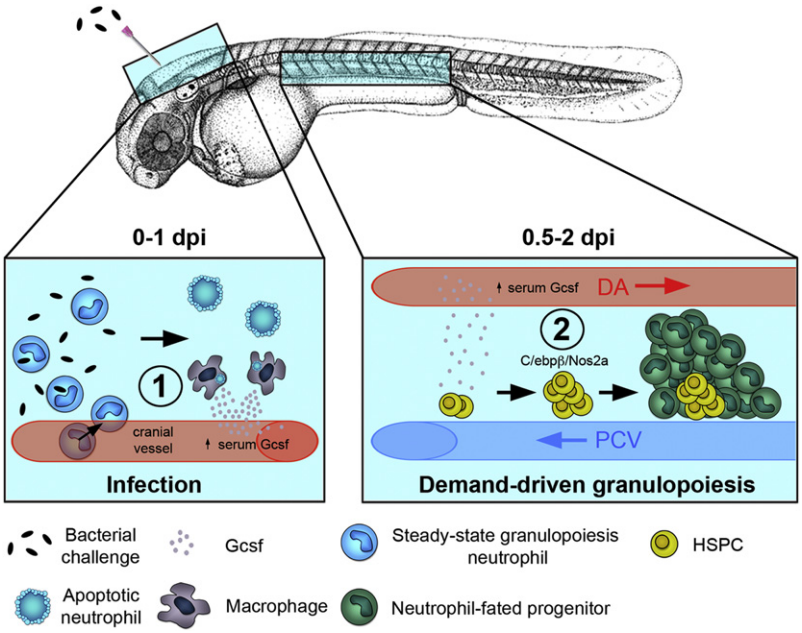

Figure 7. Proposed Model Illustrating the Reactive Capacity of the Zebrafish Blood System to Inflammatory Stress

In response to bacterial challenge, neutrophils infiltrate the infection foci to help clear bacteria before undergoing apoptosis. Macrophages then arrive to remove neutrophil debris and express the granulopoiesis-promoting cytokine Gcsf (1). Gcsf reaches the AGM compartment via the circulation to support the proliferation/expansion of HSPCs and neutrophil-fated progenitors by promoting C/ebpβ-dependent *nos2a* expression (2).

drive *nos2a* expression within zebrafish embryos. Analysis of the promoter region immediately upstream of the zebrafish *nos2a* transcription start site revealed a number of C/EBPβ consensus motifs (data not shown).

NO is a pleiotropic biomodulator in a number of systems, including the hematopoietic system. Positive and negative roles for NO during cell proliferation and steady-state blood development have been reported (Guthrie et al., 2005; Krasnov et al., 2008; Krstić et al., 2009; Michurina et al., 2004; North et al., 2009; Villalobo, 2006). In zebrafish, blood-flow-responsive *nos1 (nnos/enos)*-derived NO has been shown to contribute to *runx1*$^{+}$*cmyb*$^{+}$ HSPC development within the AGM region such that NO-donors enhance, while NO-inhibitors (and inhibitors of downstream components of NO signaling, such as ODQ) deplete, HSPC numbers (North et al., 2009). In mice, intrauterine delivery of the pan-NOS-inhibitor L-NAME blocks hematopoietic cluster formation within the AGM, strongly arguing for a conserved role for NO signaling as a positive regulator of blood stem cell development. We propose a role for infection-responsive NO, generated by Nos2a, during expansion of zebrafish HSPCs in response to inflammatory stress. Given the expression of *nos2a* within HSPCs in the AGM from 1 dpi, this source of NO likely influences neighboring blood progenitors in a paracrine fashion. We were unable to confirm these early *nos2a*-expressing cells as HSPCs by dual staining with HSPC markers due to technical limitations. However, given that these *nos2a*-expressing cells occupy the AGM, prior to the emergence of *lyz*-expressing neutrophil-fated progenitors at a time when HSPC numbers are expanding in a Nos2a-dependent manner, suggests that they are HSPCs. Despite studies examining the role of NOS2 during the immune response, a role during demand-driven granulopoiesis or infection-responsive HSPC expansion has not been described.

This study proposes a role for Nos2a-generated NO, downstream of C/ebpβ, in supporting HSPC proliferation/expansion following infection. To date, the ability to expand HSPCs ex vivo remains limited (Dahlberg et al., 2011). As such, identifying novel mechanisms that influence HSPC proliferative capacity is an area of intense interest heightened by their therapeutic relevance to both malignant and nonmalignant diseases. Additional studies are required to determine whether manipulating C/EBPβ and/or NOS2 activity influences the capacity of mammalian HSPCs and whether this newly identified pathway can be targeted for therapeutic benefit.

EXPERIMENTAL PROCEDURES

Refer to the Supplemental Information for fully detailed experimental procedures.

Zebrafish Maintenance

Zebrafish embryos obtained from natural spawnings were raised at 28°C in E3 Medium (Westerfield, 2000) and were developmentally staged as described (Kimmel et al., 1995). Transgenic reporter lines used in this study are summarized in Table S1. Research was conducted with approval from The University of Auckland Animal Ethics Committee.

QPCR

QPCR was performed with Platinum SYBR Green qPCR SuperMix-UDG with ROX (Invitrogen) using an ABI PRISM 7900HT Fast sequence detection system (Applied Biosystems) essentially as described (Oehlers et al., 2010). Gene-specific oligonucleotides were designed using Primer Express software (Table S2).

Statistical Analysis

Statistical analyses were performed using Prism 5.0 (GraphPad Software, Inc.). Statistical significance was assessed using unpaired, two-tailed t tests, and all data was presented in scatter plots with means and standard deviations.

WMISH

WMISHs were performed as described (Jowett and Lettice, 1994). Fluorescent in situ hybridization was adapted from Clay and Ramakrishnan (2005).

RT-PCR

Total RNAs were extracted from embryos and larvae using TRIzol reagent (Invitrogen) as per the manufacturer's instructions. cDNAs were then generated using Superscript III reverse transcriptase (Invitrogen). These cDNAs were used to generate gene-specific amplicons using the primer pairs listed in Table S2 (all primer pairs were designed to span at least 1 intron to control for contaminating genomic DNA).

MO Injection

MOs (Gene Tools, Philomath, OR) were resuspended and injected as described (Nasevicius and Ekker, 2000). Efficacious doses for all MOs were determined empirically. RT-PCR was used to determine MO specificity where splice-blocking MOs were used (see Table S3 for oligonucleotide sequences and doses).

Chemical Treatments

Unless otherwise stated compounds were resuspended according to the manufacturer's instructions and diluted to the indicated working concentrations such that the final DMSO concentration was 1%. Full details of the chemicals used, their targets, and manufacturer's and working concentrations are provided in Table S4.

Infection of Zebrafish Embryos and Larvae

Embryos and larvae were infected at the indicated ages with either GFP-labeled or nonlabeled *Salmonella enterica* serovar Typhimurium (Hall et al., 2007). Bacteria were delivered into the hindbrain ventricle of anaesthetized larvae, typically at 50 hpf. For a detailed description of bacteria culture conditions, injection procedure and actual cfu dose calculation, see Supplemental Experimental Procedures.

Capped RNA Synthesis

Synthetic capped RNA was synthesized using the mMESSAGE mMACHINE SP6 kit (Ambion) as per the manufacturer's instructions.

DAF-FM DA Staining of Larvae

The NO-specific fluorescent dye DAF-FM DA (Molecular Probes, Invitrogen) was used to detect endogenous NO as previously described (Lepiller et al., 2007).

Immunofluorescence

Immunofluorescence detection of fluorescent reporters was performed essentially as described (Hall et al., 2009a). For detection of EGFP, a chicken anti-GFP (Abcam) primary and goat anti-chicken Alexa Fluor 488-conjugated secondary antibody (Invitrogen) or a rabbit anti-GFP primary (Invitrogen) and goat anti-rabbit Alexa Fluor 633-conjugated secondary antibody (Invitrogen) were used.

Flow Cytometry

Flow cytometry was performed as previously described (Hall et al., 2009a).

Confocal Imaging

Live embryos and larvae were mounted for confocal imaging as previously described (Hall et al., 2009b). Images collected by confocal microscopy were processed and analyzed using Volocity 5.5 (Perkin Elmer).

SUPPLEMENTAL INFORMATION

Supplemental Information for this article includes Figures S1–S6, Tables S1–S4, and Supplemental Experimental Procedures and can be found with this article online at doi:10.1016/j.stem.2012.01.007.

ACKNOWLEDGMENTS

We thank Annie Chien, Sophie Wicker, Pauline Misa, Alisha Malik, and Alhad Mahagaonkar for excellent technical assistance. We also thank Nick Trede and Len Zon for supplying reporter lines and Graham Lieschke for supplying probe templates. Funding for this work was provided by a grant awarded to P.C. from the Ministry of Science & Innovation, New Zealand.

Received: August 17, 2011
Revised: December 10, 2011
Accepted: January 17, 2012
Published: February 2, 2012

REFERENCES

Adamo, L., Naveiras, O., Wenzel, P.L., McKinney-Freeman, S., Mack, P.J., Gracia-Sancho, J., Suchy-Dicey, A., Yoshimoto, M., Lensch, M.W., Yoder, M.C., et al. (2009). Biomechanical forces promote embryonic haematopoiesis. Nature *459*, 1131–1135.

Akagi, T., Saitoh, T., O'Kelly, J., Akira, S., Gombart, A.F., and Koeffler, H.P. (2008). Impaired response to GM-CSF and G-CSF, and enhanced apoptosis in C/EBPbeta-deficient hematopoietic cells. Blood *111*, 2999–3004.

Baldridge, M.T., King, K.Y., Boles, N.C., Weksberg, D.C., and Goodell, M.A. (2010). Quiescent haematopoietic stem cells are activated by IFN-gamma in response to chronic infection. Nature *465*, 793–797.

Baldridge, M.T., King, K.Y., and Goodell, M.A. (2011). Inflammatory signals regulate hematopoietic stem cells. Trends Immunol. *32*, 57–65.

Bertrand, J.Y., Chi, N.C., Santoso, B., Teng, S., Stainier, D.Y., and Traver, D. (2010). Haematopoietic stem cells derive directly from aortic endothelium during development. Nature *464*, 108–111.

Clay, H., and Ramakrishnan, L. (2005). Multiplex fluorescent in situ hybridization in zebrafish embryos using tyramide signal amplification. Zebrafish *2*, 105–111.

Dahlberg, A., Delaney, C., and Bernstein, I.D. (2011). Ex vivo expansion of human hematopoietic stem and progenitor cells. Blood *117*, 6083–6090.

Ellett, F., Pase, L., Hayman, J.W., Andrianopoulos, A., and Lieschke, G.J. (2011). mpeg1 promoter transgenes direct macrophage-lineage expression in zebrafish. Blood *117*, e49–e56.

Guo, Z., Shao, L., Feng, X., Reid, K., Marderstein, E., Nakao, A., and Geller, D.A. (2003). A critical role for C/EBPbeta binding to the AABS promoter response element in the human iNOS gene. FASEB J. *17*, 1718–1720.

Guthrie, S.M., Curtis, L.M., Mames, R.N., Simon, G.G., Grant, M.B., and Scott, E.W. (2005). The nitric oxide pathway modulates hemangioblast activity of adult hematopoietic stem cells. Blood *105*, 1916–1922.

Hall, C., Flores, M.V., Storm, T., Crosier, K., and Crosier, P. (2007). The zebrafish lysozyme C promoter drives myeloid-specific expression in transgenic fish. BMC Dev. Biol. *7*, 42.

Hall, C., Flores, M.V., Chien, A., Davidson, A., Crosier, K., and Crosier, P. (2009a). Transgenic zebrafish reporter lines reveal conserved Toll-like receptor signaling potential in embryonic myeloid leukocytes and adult immune cell lineages. J. Leukoc. Biol. *85*, 751–765.

Hall, C., Flores, M.V., Crosier, K., and Crosier, P. (2009b). Live cell imaging of zebrafish leukocytes. Methods Mol. Biol. *546*, 255–271.

Hirai, H., Zhang, P., Dayaram, T., Hetherington, C.J., Mizuno, S., Imanishi, J., Akashi, K., and Tenen, D.G. (2006). C/EBPbeta is required for 'emergency' granulopoiesis. Nat. Immunol. *7*, 732–739.

Jowett, T., and Lettice, L. (1994). Whole-mount in situ hybridizations on zebrafish embryos using a mixture of digoxigenin- and fluorescein-labelled probes. Trends Genet. *10*, 73–74.

Kastan, M.B., Slamon, D.J., and Civin, C.I. (1989). Expression of protooncogene c-myb in normal human hematopoietic cells. Blood *73*, 1444–1451.

Kaushansky, K. (2006). Lineage-specific hematopoietic growth factors. N. Engl. J. Med. *354*, 2034–2045.

Kimmel, C.B., Ballard, W.W., Kimmel, S.R., Ullmann, B., and Schilling, T.F. (1995). Stages of embryonic development of the zebrafish. Dev. Dyn. *203*, 253–310.

King, K.Y., and Goodell, M.A. (2011). Inflammatory modulation of HSCs: viewing the HSC as a foundation for the immune response. Nat. Rev. *11*, 685–692.

Kissa, K., and Herbomel, P. (2010). Blood stem cells emerge from aortic endothelium by a novel type of cell transition. Nature *464*, 112–115.

Korhonen, R., Lahti, A., Kankaanranta, H., and Moilanen, E. (2005). Nitric oxide production and signaling in inflammation. Curr. Drug Targets Inflamm. Allergy *4*, 471–479.

Krasnov, P., Michurina, T., Packer, M.A., Stasiv, Y., Nakaya, N., Moore, K.A., Drazan, K.E., and Enikolopov, G. (2008). Neuronal nitric oxide synthase contributes to the regulation of hematopoiesis. Mol. Med. *14*, 141–149.

Krstić, A., Ilić, V., Mojsilović, S., Jovcić, G., Milenković, P., and Bugarski, D. (2009). p38 MAPK signaling mediates IL-17-induced nitric oxide synthase expression in bone marrow cells. Growth Factors *27*, 79–90.

Lam, E.Y., Chau, J.Y., Kalev-Zylinska, M.L., Fountaine, T.M., Mead, R.S., Hall, C.J., Crosier, P.S., Crosier, K.E., and Flores, M.V. (2009). Zebrafish runx1 promoter-EGFP transgenics mark discrete sites of definitive blood progenitors. Blood *113*, 1241–1249.

Lam, E.Y., Hall, C.J., Crosier, P.S., Crosier, K.E., and Flores, M.V. (2010). Live imaging of Runx1 expression in the dorsal aorta tracks the emergence of blood progenitors from endothelial cells. Blood *116*, 909–914.

Le Guyader, D., Redd, M.J., Colucci-Guyon, E., Murayama, E., Kissa, K., Briolat, V., Mordelet, E., Zapata, A., Shinomiya, H., and Herbomel, P. (2008). Origins and unconventional behavior of neutrophils in developing zebrafish. Blood *111*, 132–141.

Lepiller, S., Laurens, V., Bouchot, A., Herbomel, P., Solary, E., and Chluba, J. (2007). Imaging of nitric oxide in a living vertebrate using a diamino-fluorescein probe. Free Radic. Biol. Med. *43*, 619–627.

Lepiller, S., Franche, N., Solary, E., Chluba, J., and Laurens, V. (2009). Comparative analysis of zebrafish nos2a and nos2b genes. Gene *445*, 58–65.

Lieschke, G.J., Oates, A.C., Paw, B.H., Thompson, M.A., Hall, N.E., Ward, A.C., Ho, R.K., Zon, L.I., and Layton, J.E. (2002). Zebrafish SPI-1 (PU.1) marks a site of myeloid development independent of primitive erythropoiesis: implications for axial patterning. Dev. Biol. *246*, 274–295.

Lyons, S.E., Shue, B.C., Oates, A.C., Zon, L.I., and Liu, P.P. (2001). A novel myeloid-restricted zebrafish CCAAT/enhancer-binding protein with a potent transcriptional activation domain. Blood *97*, 2611–2617.

Meijer, A.H., van der Sar, A.M., Cunha, C., Lamers, G.E., Laplante, M.A., Kikuta, H., Bitter, W., Becker, T.S., and Spaink, H.P. (2008). Identification and real-time imaging of a myc-expressing neutrophil population involved in inflammation and mycobacterial granuloma formation in zebrafish. Dev. Comp. Immunol. *32*, 36–49.

Michurina, T., Krasnov, P., Balazs, A., Nakaya, N., Vasilieva, T., Kuzin, B., Khrushchov, N., Mulligan, R.C., and Enikolopov, G. (2004). Nitric oxide is a regulator of hematopoietic stem cell activity. Mol. Ther. *10*, 241–248.

Motoyoshi, K. (1998). Biological activities and clinical application of M-CSF. Int. J. Hematol. *67*, 109–122.

Murayama, E., Kissa, K., Zapata, A., Mordelet, E., Briolat, V., Lin, H.F., Handin, R.I., and Herbomel, P. (2006). Tracing hematopoietic precursor migration to successive hematopoietic organs during zebrafish development. Immunity *25*, 963–975.

Nasevicius, A., and Ekker, S.C. (2000). Effective targeted gene 'knockdown' in zebrafish. Nat. Genet. *26*, 216–220.

North, T.E., Goessling, W., Walkley, C.R., Lengerke, C., Kopani, K.R., Lord, A.M., Weber, G.J., Bowman, T.V., Jang, I.H., Grosser, T., et al. (2007). Prostaglandin E2 regulates vertebrate haematopoietic stem cell homeostasis. Nature *447*, 1007–1011.

North, T.E., Goessling, W., Peeters, M., Li, P., Ceol, C., Lord, A.M., Weber, G.J., Harris, J., Cutting, C.C., Huang, P., et al. (2009). Hematopoietic stem cell development is dependent on blood flow. Cell *137*, 736–748.

Oehlers, S.H., Flores, M.V., Hall, C.J., O'Toole, R., Swift, S., Crosier, K.E., and Crosier, P.S. (2010). Expression of zebrafish cxcl8 (interleukin-8) and its receptors during development and in response to immune stimulation. Dev. Comp. Immunol. *34*, 352–359.

Panopoulos, A.D., and Watowich, S.S. (2008). Granulocyte colony-stimulating factor: molecular mechanisms of action during steady state and 'emergency' hematopoiesis. Cytokine *42*, 277–288.

Rezzoug, F., Huang, Y., Tanner, M.K., Wysoczynski, M., Schanie, C.L., Chilton, P.M., Ratajczak, M.Z., Fugier-Vivier, I.J., and Ildstad, S.T. (2008). TNF-alpha is critical to facilitate hemopoietic stem cell engraftment and function. J. Immunol. *180*, 49–57.

Scumpia, P.O., Kelly-Scumpia, K.M., Delano, M.J., Weinstein, J.S., Cuenca, A.G., Al-Quran, S., Bovio, I., Akira, S., Kumagai, Y., and Moldawer, L.L. (2010). Cutting edge: bacterial infection induces hematopoietic stem and progenitor cell expansion in the absence of TLR signaling. J. Immunol. *184*, 2247–2251.

Takizawa, H., Regoes, R.R., Boddupalli, C.S., Bonhoeffer, S., and Manz, M.G. (2011). Dynamic variation in cycling of hematopoietic stem cells in steady state and inflammation. J. Exp. Med. *208*, 273–284.

Teng, X., Li, D., Catravas, J.D., and Johns, R.A. (2002). C/EBP-beta mediates iNOS induction by hypoxia in rat pulmonary microvascular smooth muscle cells. Circ. Res. *90*, 125–127.

Trumpp, A., Essers, M., and Wilson, A. (2010). Awakening dormant haematopoietic stem cells. Nat. Rev. *10*, 201–209.

Ueda, Y., Kondo, M., and Kelsoe, G. (2005). Inflammation and the reciprocal production of granulocytes and lymphocytes in bone marrow. J. Exp. Med. *201*, 1771–1780.

Villalobo, A. (2006). Nitric oxide and cell proliferation. FEBS J. *273*, 2329–2344.

Westerfield, M. (2000). The zebrafish book. A guide for the laboratory use of zebrafish (Danio rerio), Fourth Edition (Eugene: Univ. of Oregon Press).

Willett, C.E., Kawasaki, H., Amemiya, C.T., Lin, S., and Steiner, L.A. (2001). Ikaros expression as a marker for lymphoid progenitors during zebrafish development. Dev. Dyn. *222*, 694–698.

Zhang, H., Nguyen-Jackson, H., Panopoulos, A.D., Li, H.S., Murray, P.J., and Watowich, S.S. (2010). STAT3 controls myeloid progenitor growth during emergency granulopoiesis. Blood *116*, 2462–2471.